Journal of Structural Geology, Vol. 12, No. 8, pp. 1047 to 1059, 1990
Printed in Great Britain

0191-8141/90 $03.00 + 0.00

Least-squares center-to-center and mean object ellipse fabric analysis

ERIC A. ERSLEV and HONGXING GE

Department of Earth Resources, Colorado State University, Fort Collins, CO 80523, U.S.A.

(*Received* 13 *June* 1989; *accepted in revised form* 28 *February* 1990)

Abstract—The subjectivity of ellipse fitting in many strain techniques has hindered the determination of fabric anisotropy and tectonic strain. However, many sets of x, y co-ordinates can be approximated as an ellipse using a least-squares algorithm to calculate a best-fit ellipse and associated average radial error. For instance, the two dimensional shape of many objects can be approximated as an ellipse by entering digitized co-ordinates of the object margin into the ellipse algorithm.

The rim of maximum point density in a normalized Fry diagram is defined by normalized center-to-center distances between touching or nearly touching objects. The enhanced normalized Fry (ENFry) method automates ellipse fitting by entering center-to-center distances between these 'touching' objects into the least-squares ellipse algorithm. For homogeneously deformed populations of 200 objects, the ENFry method gives an accurate and precise measure of whole-rock fabric anisotropy, particularly for low ellipticities. When matrix strain exceeds clast strain, manual ellipse fitting of normalized Fry plots gives more accurate matrix anisotropies.

The mean object ellipse (MOE) method calculates the best-fit ellipse from the geometry of the objects. Three points from the margin of each object ellipse, centered at the origin and expanded or reduced to unit volume, are used to calculate the best-fit fabric ellipse. The MOE method is very precise for small data sets, making it a good method for mapping heterogeneous object strain. However, least-squares calculations maximize the influence of distal and spurious ellipticities, causing the MOE method to overestimate the fabric ellipticity of most aggregates.

INTRODUCTION

QUANTITATIVE analysis of rock fabric can provide important constraints on many petrogenetic problems. Structural geologists have traditionally used fabric anisotropy to quantify deformation histories of tectonites (e.g. Cloos 1947, Ramsay 1967, Schmid *et al.* 1987). Whilst these strain methods are not inherently limited to the measurement of deformation, quantitative evaluation of subtle fabric anisotropy formed by mild deformation, compaction and depositional alignment is hindered by the coarse resolution and subjectivity of many strain methods.

In addition, the lack of automated ellipse calculation and quantitative error determination prevents the establishment of accuracy and precision standards. For instance, evaluation of object strain by plotting object ellipticity against long axis inclination (R_f/ϕ technique: Ramsay 1967, Lisle 1985) typically involves determining the top and bottom of an onion-like shape encompassing most of the data in an R_f/ϕ diagram. The selection of objects to include and objects to exclude can be very arbitrary.

Measuring center-to-center strain from scatter plots of center-to-center distances is usually even more subjective. Determining the level of maximum point density in the Ramsay (1967) technique, where inclinations of center-to-center distances are plotted against the actual distances, is matched in difficulty with determining the rim of maximum point density in a Fry (1979) plot (Fig. 1a). Both methods require an unrealistic degree of two-dimensional anticlustering, which is inherently limited in packed aggregates. Even a two-dimensional plane through an aggregate with perfect three-dimensional anticlustering (e.g. packed, equi-volume spheres) contains variably sized cross-sections through both the middle and ends of the objects (Bhattacharyya & Longiaru 1986, Erslev 1988). This effect, when combined with normal sorting, limits anticlustering and obscures the fabric ellipse.

In packed aggregates, plotting the normalized distances between object centers (actual distance divided by the sum of the average radii of the two objects) in the normalized Fry diagram (Fig. 1b) (Erslev 1988) provides a clearer definition of the fabric ellipse by reducing the number of points inside the rim of maximum point density. In packed objects, the rim of maximum point density is defined by touching (or nearly touching) objects irrespective of their two-dimensional size. Since the normalized Fry method is not dependent on two-dimensional anticlustering, it should be independent of sorting, which can further decrease the anticlustering of packed aggregates.

However, the normalized Fry method still requires manual ellipse fitting, introducing a subjective, irreproducible step to the analysis. We have found that students in structural geology classes are often difficult to convince that the 'answer' ellipse is significantly better than theirs. In complex natural aggregates, variable initial and tectonic ellipticities broaden the rim of maximum point density, making ellipse fitting even more difficult.

The fabric methods proposed by this paper allow analytical, unbiased determination of individual object and overall fabric anisotropy. The analyses are implemented using a least-squares ellipse-fitting algorithm in specially modified versions of INSTRAIN 2.5, an inte-

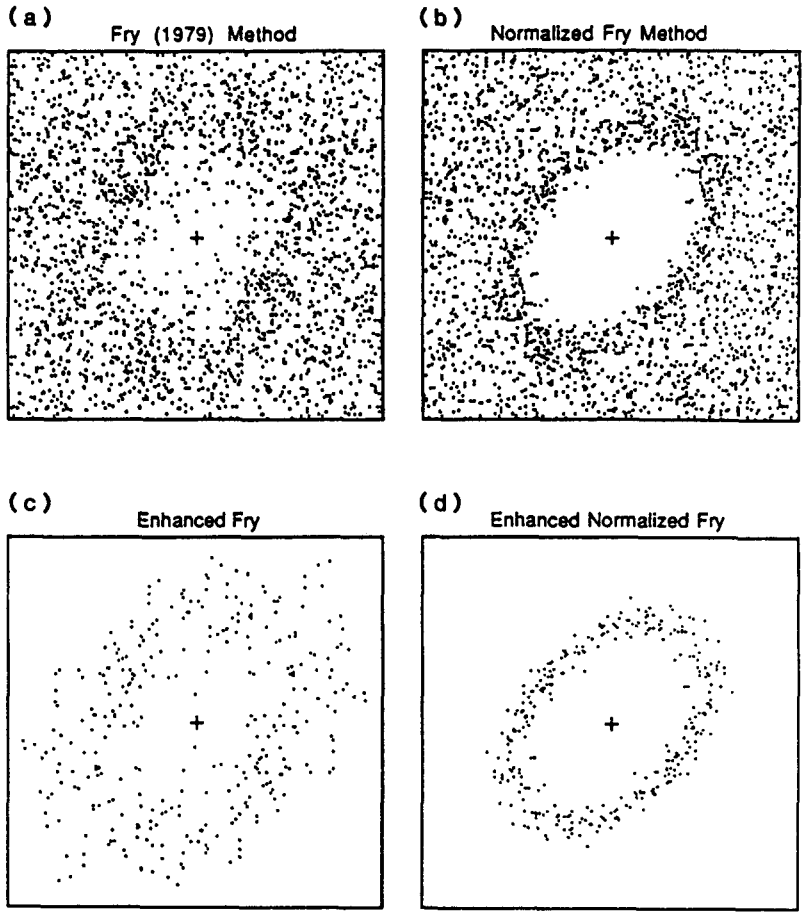

Fig. 1. (a) Fry (1979) all–object–object separations, (b) normalized Fry (Erslev 1988), (c) enhanced Fry (EFry) and (d) enhanced normalized Fry (ENFry) plots with least-squares best-fit ellipses and their associated errors for the aggregate from fig. 5.7 in Ramsay & Huber (1983).

grated fabric analysis program for IBM-PC compatible and Macintosh computers. This paper will derive a least-squares algorithm for a best-fit ellipse centered at the origin, propose new methods of fabric analysis using this algorithm and test the precision and accuracy of the methods.

LEAST-SQUARES FABRIC ANALYSIS METHODS

The classical approach to quantifying the two-dimensional geometry of textural elements in a material (e.g. grain dimension or aggregate geometry) is to calculate a fabric ellipse measuring the deviation from an ideal initial state approximated by a circular geometry (Ramsay 1967). This requires the graphical or mathematical estimation of a best-fit ellipse. Calculation of a best-fit ellipse allows the reproducibility necessary if standards of precision and accuracy are to be established. Current line strain (Panozzo 1984, Schmid *et al.* 1987), mean ellipticity (Ramsay 1967) and mean ellipse (Shimamoto & Ikeda 1976) methods give unique values of ellipticity independent of analyst bias but lack direct error calculations.

Another approach is to minimize an error equation quantifying the deviation of the observations from a best-fit ellipse. The standard least-squares method was used in this analysis because the solution of the least-squares equations gives a unique, unbiased result. The least-squares derivation for an ellipse centered at the origin is given in the Appendix. Some of the shortcomings of least-squares methods are illustrated and discussed later in this paper. Other options involving the iterative minimization of error equations are currently being evaluated.

In order to measure the closeness of the data to the calculated best-fit ellipse, the average radial error is calculated for each least-squares ellipse. In this pro-

cedure, the distance between the ellipse center (at the origin) and data point is compared with the predicted distance between the ellipse center and the ellipse margin on the line including the data point. The predicted distance is calculated by combining the ellipse equation with the equation for the line from the center to the data point. The absolute value of the difference between these distances is divided by the predicted distance, yielding the error for a specific data point. The errors are summed for all points and divided by the number of points, giving the average radial error.

The following methods of fabric analysis use least-squares ellipse (Appendix) and error algorithms, implemented in PASCAL subroutines, to calculate the size, ellipticity and inclination of the best-fit ellipse.

Least-squares object digitizing

Accurate fabric analysis presumes the collection of accurate, reproducible object shape data. The definition of elliptical objects using four points at the end-points of the principal axes of an ellipse requires the manual determination of an average or inscribed ellipse for each object, adding subjectivity and time. Digitizing five points on the margin of the object, with the computer calculating the conic uniquely defined by the points, is faster, particularly for elliptical aggregates like strained ooids, but assumes that the selected five points are representative. The selection of representative points is particularly problematical for objects with planar or cuspate grain boundaries.

To increase the accuracy of individual object descriptions, the least-squares algorithm (Appendix) was used in a digitizing program which approximates object outlines as ellipses. The program collects points on the margin of an object as it is traced in increment mode. These points are translated toward the origin by subtracting the centroid co-ordinates (average x, y) from each co-ordinate. The translated co-ordinates are entered into the least-squares ellipse algorithm (Appendix) to define the best-fit ellipse.

One motivation for incorporating the least-squares ellipse algorithm in a digitizer program was to check the algorithm for errors and rotational invariance, which was a problem with an earlier least-squares formulation. Tests, including digitizing ellipse templates, deforming points by synthetic simple shear and rotating points in a spreadsheet, gave the expected ellipticities, indicating no significant deviations or rotational variability (Ge 1990). The comparison of results from least-squares digitizing with earlier results from manual four-point and five-point digitizing shows increased consistency, suggesting improved accuracy.

The number of points required for accurate estimation of the best-fit ellipse depends on the angularity of the object. Three objects, a slightly pear-shaped ooid, a six-sided quartz polygon and a triangular quartz grain were digitized 20 times using different increments between data points (Fig. 2). These increments gave between five and 44 points on the margin of the objects, with smaller increments giving larger numbers of points. For each increment and grain shape, the standard deviation of 20 least-squares ellipticities was calculated to evaluate the effect of different numbers of points on the determination of the best-fit ellipse. For all three grain shapes, the standard deviation of ellipticity increased dramatically for larger increments, which gave fewer points per grain margin. The difference in precision between the angular, triangular grain and the more equant grains reflects the greater deviations from an ideal ellipse at grain asperities, which may not be represented in large increment grain digitizing. This analysis suggests that the digitizing increment should be set to allow 25 points per grain to allow accurate approximation of irregular grains as ellipses.

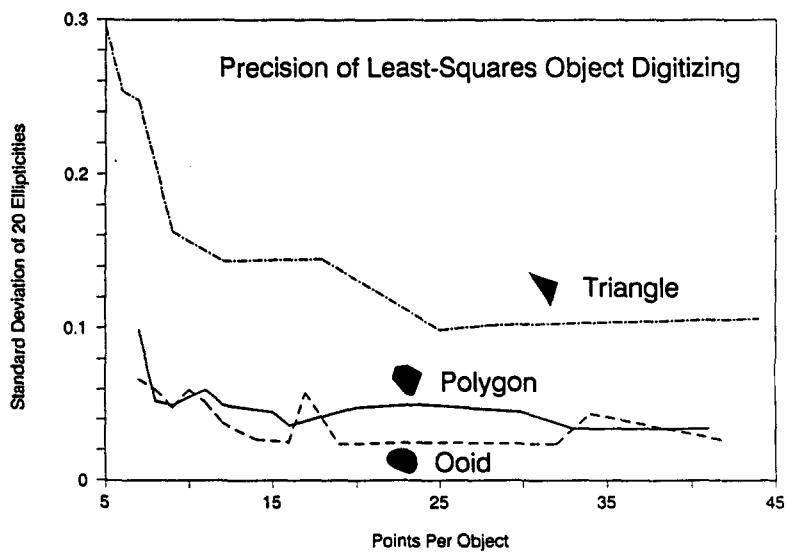

Fig. 2. The reproducibility of least-squares ellipse definitions based on different numbers of digitized points on the margins of three grain shapes.

Enhanced Fry (EFry) and enhanced normalized Fry (ENFry) methods

The Fry (1979) and normalized Fry (Erslev 1988) methods offer a graphical approach to center-to-center fabric analysis (Figs. 1a & b). Fry (1979) plots are an elegant way to analyze anisotropy in anticlustered populations but the lack of sufficient two-dimensional anticlustering in most aggregates makes ellipse selection difficult. The increased point density contrast in normalized Fry diagrams (Erslev 1988) facilitates the selection of a fabric ellipse. However, manual ellipse fitting to the rim of a maximum point density is still required.

Ideally, we would like to eliminate, in an unbiased way, all points except those contributing to the rim of maximum point density. The problem with quantifying the Fry technique is the lack of logical, non-subjective criteria to eliminate distances which do not contribute to the rim of maximum point density. Restricting the size range of object cross-sections used to define centers does clean out the central region of standard Fry plots, but this also reduces the number of nearest neighbors for a given data set. In an attempt to clarify the rim of maximum point density, Crespi (1986) eliminated distances below a minimum center-to-center distance, but this makes the inner void more circular. In addition, no unbiased criteria exist for removing center-to-center distances which plot outside the rim of maximum point density.

For homogeneously deformed, packed aggregates, the rim of maximum point density in normalized Fry plots consists of distances between touching or nearly touching neighbors. The following, synthetic example of a two-dimensional, undeformed aggregate of circular objects illustrates this relationship. The normalized distance (D_n) between objects a and b equals the actual center-to-center distance D divided by the sum of their radii. Since these objects cannot overlap and each object has perfectly circular cross-sections, the minimum D_n (1.0) is defined by touching pairs of objects. For this undeformed case, the rim of maximum point density in a normalized Fry plot starts at a distance $D_n = 1.0$, which is defined by touching circular cross-sections. For deformed, elliptical objects, object radii are variable so the average radius for each object ($R = (X/2 * Y/2)^{1/2}$, where X and Y are the long and short axes of the ellipse) must be defined. The deformed case is simply related to the undeformed case by a stretch factor, which does not affect the validity of this argument (see equations 4 in Erslev 1988).

Thus, for packed aggregates, the rim of maximum point density in a normalized Fry diagram is defined by objects in or nearly in contact with each other. These pairs of 'touching' objects can be manually selected by entering pairs of approximate center locations. However, this adds a subjective step which might bias the analysis. Alternatively, touching pairs can be computer selected by comparing the center-to-center distance (D) between each pair of objects with the sum of object radii for each pair ($r_a + r_b$) measured parallel to D. These radii are elliptical radii measured on the line between the two centers in question, not average radii used to normalize the distances. Dividing the center-to-center distance by the sum of these elliptical radii ($D/(r_a + r_b)$) gives an object-pair selection factor (or selection factor for short) which allows an adjustable criterion for selecting object pairs. For example, a selection factor of 1.0 will only accept pairs whose $D/(r_a + r_b) \leq 1.0$. These pairs include elliptical objects in contact with each other and objects whose defining ellipses overlap. This is common in polygonal aggregates with interpenetrating grain boundaries.

The normalized center-to-center distances between 'touching' pairs, as defined by the object pair selection factor or by manual identification of nearest-neighbors, can be plotted in an enhanced normalized Fry (or ENFry) plot (Fig. 1d). The true center-to-center distances can also be plotted in an enhanced Fry (or EFry) plot (Fig. 1c). However, the rim of maximum point density in a Fry plot is not uniquely defined by touching objects so this diagram must be interpreted carefully. The selected center-to-center and normalized center-to-

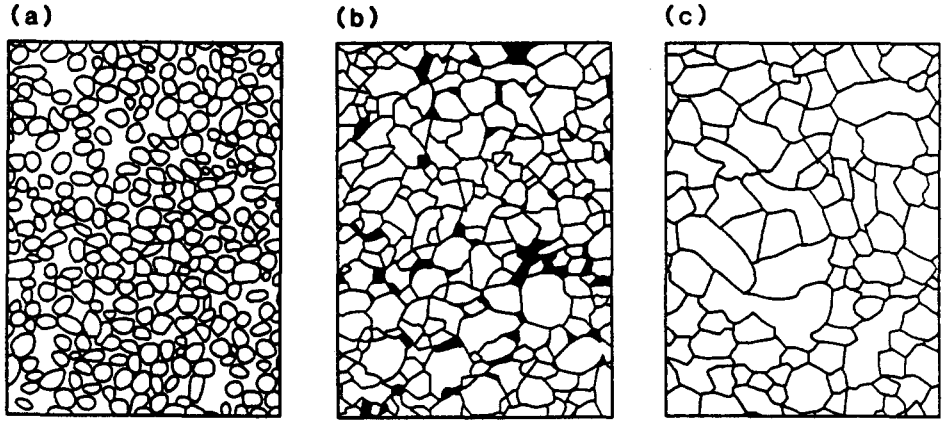

Fig. 3. Tracings of representative portions from thin sections with at least 1500 objects used for tests of precision and method variables. These samples come from (a) oolitic Ingleside Formation of Permian age from northwest of Fort Collins, Colorado, (b) Cambrian Flathead Sandstone from the northern Teton Range and (c) upper amphibolite facies quartzite of Archean age from the southwestern Beartooth Mountains.

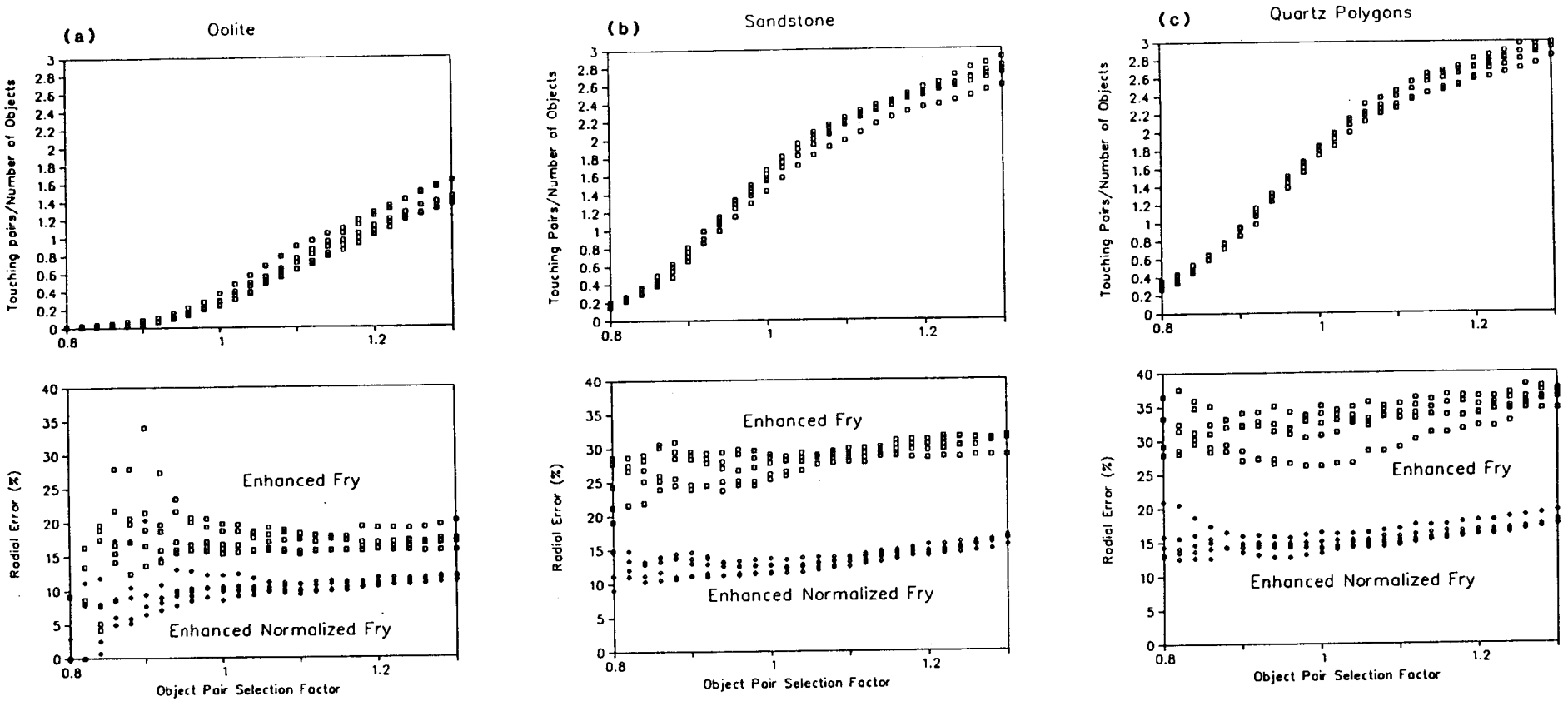

Fig. 4. The number of touching pairs and average radial error plotted vs selection factor for the aggregates illustrated in Fig. 3.

center distances from 'touching' objects can now be entered into the least-squares ellipse algorithm which provides an unbiased estimation of ellipticity, long axis inclination and average radial error for both the EFry and ENFry methods.

In order to determine the range of optimum selection factors, data sets of 1500 objects from minimally deformed samples (Fig. 3) were digitized using the least-squares program and the smallest digitizing increment, ensuring at least 25 points per object. These aggregates were selected to represent the spectrum of packed aggregates, ranging from well-rounded, undeformed oolites to polygonal quartz in an upper amphibolite facies quartzite. The samples show no obvious fabric heterogeneity in thin section. Data files were checked for anomalous data using R_f/ϕ plots. Objects with ellipticities greater than 1 above the next largest ellipticity were eliminated from the data sets.

The number of 'touching' pairs selected is a function of the selection factor and the aggregate type (Fig. 4). Increasing the selection factor increases the number of 'touching' pairs chosen for the calculation of the best-fit ellipse and average radial error. Elliptical objects like the ooids in Fig. 3(a) require higher selection factors than the polygonal quartz grains in Fig. 3(c) to get equivalent numbers of 'touching' pairs because ooids have less object interpenetration and resulting overlap of elliptical object approximations. In many cases, each aggregate must be evaluated separately for the optimum selection factor.

For ooids, the average radial error from the enhanced normalized Fry method is highly variable at selection factors less than 1.0, stays level between 1.0 and 1.1 and then increases (Fig. 4a). The scatter at low selection factors is the result of the small number of object pairs selected. Increasing errors at selection factors above 1.1 result from decreased point density beyond the rim of maximum point density in a normalized Fry plot, resulting in a larger spread of x, y co-ordinates. The same basic patterns occur in the sandstone and polygonal quartz aggregates, but at lower selection factors because of more object interpenetration (Figs. 4b & c).

Another approach to choosing the optimal selection factor is to determine how many touching pairs should be expected for the objects if they originated as a close-packed aggregate. Synthetic aggregates of equi-volume spheres in Erslev (1988) had 0.60 touching pairs per object. Packed spheres in Chilingarian & Wolf (1975) had 0.63 touching pairs per grain. Samples of lead shot with variable sorting had 0.63, 0.57 and 0.55 touching pairs per object. Thus, for an aggregate of originally close-packed objects, approximately 0.6 touching pairs per object should be selected by varying the selection factor. In general, concave-inward objects like ooids or poorly cemented sand grains require selection factors between 1.0 and 1.1 whereas polygonal aggregates require selection factors between 0.9 and 1.0.

Non-close packed aggregates with abundant matrix material will yield fewer 'touching' pairs for a given selection factor. In this case, the analyst should estimate the number of touching pairs visually and adjust the selection factor to give that number of pairs.

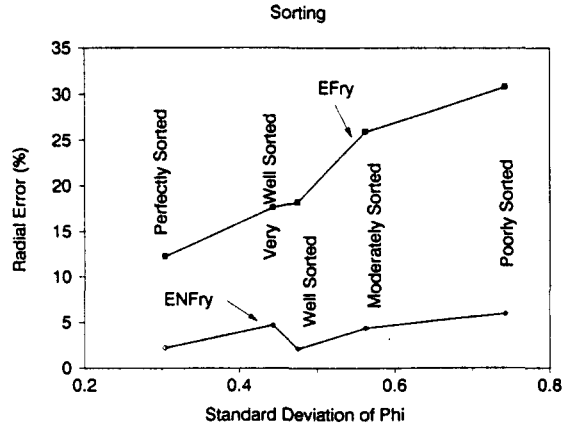

Fig. 5. Sorting, as measured on the analyzed plane by the standard deviation of ϕ (Folk 1974), plotted vs average radial error given by the enhanced Fry (EFry) and enhanced normalized Fry methods (ENFry).

One advantage of normalized Fry techniques over Fry techniques is that they appear to be independent of sorting. This hypothesis was tested using the aggregates of spheres from Erslev (1988) and three aggregates of variably-sized lead shot. Sorting was calculated using the standard deviation of the object ϕ derived from object areas on the two-dimensional surface (Folk 1974, Ge 1990). Figure 5 shows that the average radial error of the enhanced Fry method increases dramatically with decreased sorting. The average radial error of the enhanced normalized Fry method remains roughly the same regardless of sorting, with the aggregates of slightly elliptical lead shot giving higher errors than aggregates of spheres. This experiment confirms that normalized Fry techniques are independent of sorting.

Mean object ellipse (MOE) method

The calculation of mean ellipticities is one of the oldest techniques for quantifying strain. Ramsay (1967), Dunnet (1969) and Lisle (1977) have shown the utility of arithmetic, geometric and harmonic mean ellipticities despite their tendency to overestimate the ellipticity, particularly for minimal fabric anisotropies.

The reason for this error is illustrated in Figs. 6(a) & (b). If an aggregate of undeformed objects has equivalent yet randomly oriented initial ellipticity, mean ellipticities will be closer to the initial ellipticity (1.5) than the tectonic ellipticity (1.0). Because mean ellipticities ignore the effect of long axis orientation (ϕ), they do not fully characterize the geometry of the fabric anisotropy.

An alternative method, the mean object ellipse (MOE) method, is illustrated in Fig. 6(c). MOE calculates the least-squares best-fit ellipse from the shape of objects, which are input as ellipses, by combining their shapes into a single, average ellipse. First, the center of the ellipse approximating each object is translated to the origin. In order to remove size effects, the object area is normalized to a constant value, effectively expanding or shrinking the object without distorting its shape. Since a

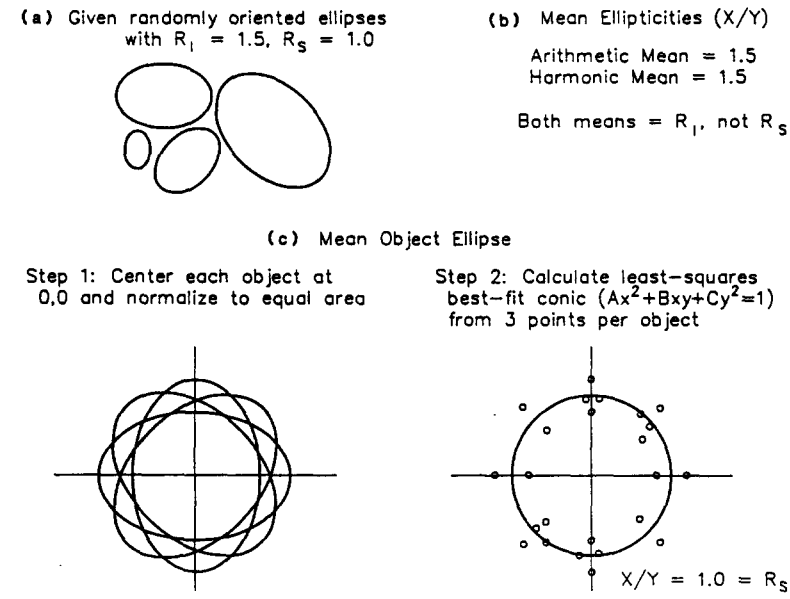

Fig. 6. Graphical illustration of the difference between (b) mean ellipticity and (c) mean object ellipse calculations. For clarity, the diagram in Step 2 of (c) plots three points per object plus their symmetric equivalents, giving a total of six points per object.

centered ellipse is uniquely characterized by three points on its margin, the program (1) rotates the principal ellipse axis parallel to the x co-ordinate axis, (2) calculates the end-points of the maximum and minimum ellipse axes and an intermediate point on the ellipse at x equal to one half the maximum stretch, and (3) rotates the three points back to their original position. The three non-centrosymmetric points for each object are input into the least-squares and error procedures to determine the mean object ellipse. These routines output the best-fit ellipticity, long axis angle (ϕ) and associated average radial error for the entire aggregate. This method is similar to the mean ellipse calculations of Shimamoto & Ikeda (1976) who calculated the ellipse equation for each object and then averaged the coefficients.

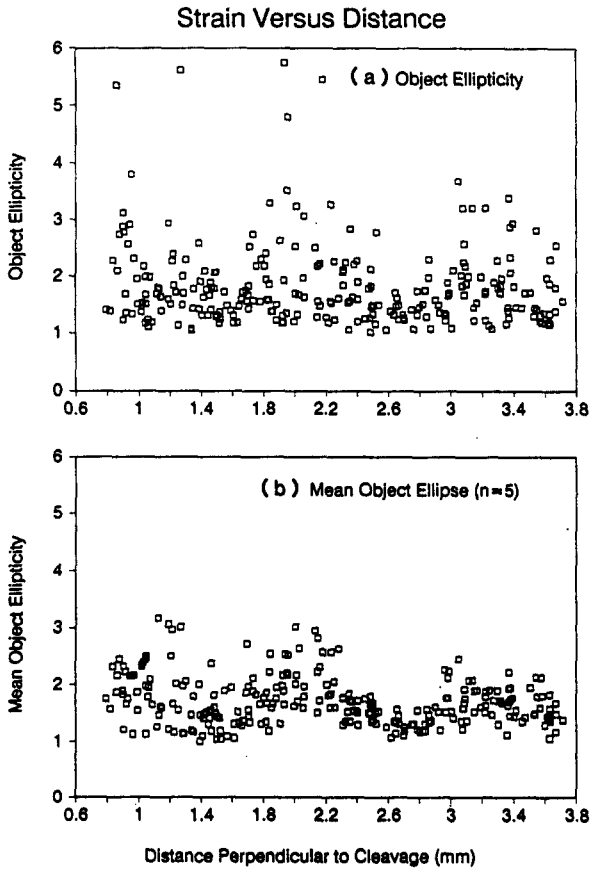

Fig. 7. Evaluation of the heterogeneous strain in spaced cleavage cutting a quartz arenite in Powell (1982). Distance is measured from the bottom of the photomicrograph in Powell (1982), with cleavage zones at 1.2, 2.1 and 3.2 mm.

The MOE method is ideally suited for the creation of smoothed strain maps by calculating the mean object ellipse for the nearest neighbors of each object. Figure 7 shows two ellipticity profiles through a quartzite cut by three cleavage zones (Powell 1982). Both individual object ellipticity (Fig. 7a) and MOE (calculated for the nearest five objects and plotted in Fig. 7b) show higher ellipticities in the three cleavage zones. The variability of the raw ellipticity values is smoothed out by the averaging effect of the MOE ellipticity.

PRECISION AND ACCURACY OF EFRY, ENFRY AND MOE METHODS

The precision (reproducibility) of the new fabric techniques was tested on natural aggregates using four data sets of 1500 objects from the minimally deformed samples illustrated in Fig. 3. The selection factor was chosen to allow approximately 0.6 'touching' pairs per object. The digitized object data were entered into a modified version of INSTRAIN which outputs fabric data to a disk file for non-overlapping subsets of objects. The number of objects per subset was incremented by 25 from 25 to 600, the maximum allowed by the program.

Figures 8 and 9 show the variations of average radial error, long axis inclination and ellipticity for the EFry, MOE and ENFry methods with different data subset

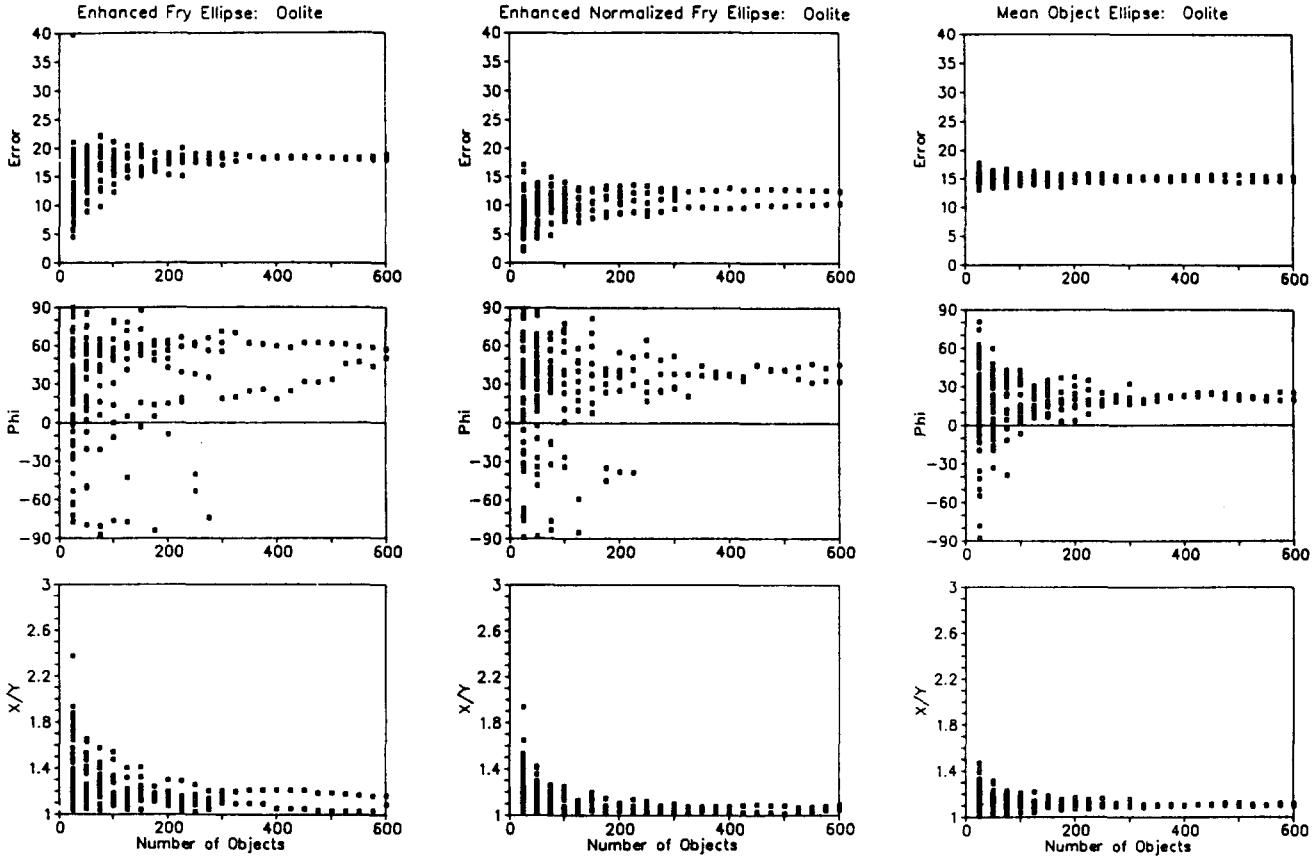

Fig. 8. Scatter plots of average radial error, long axis inclination and ellipticity for EFry, ENFry and MOE ellipse determinations using non-overlapping subsets of the oolitic aggregate illustrated in Fig. 3(a).

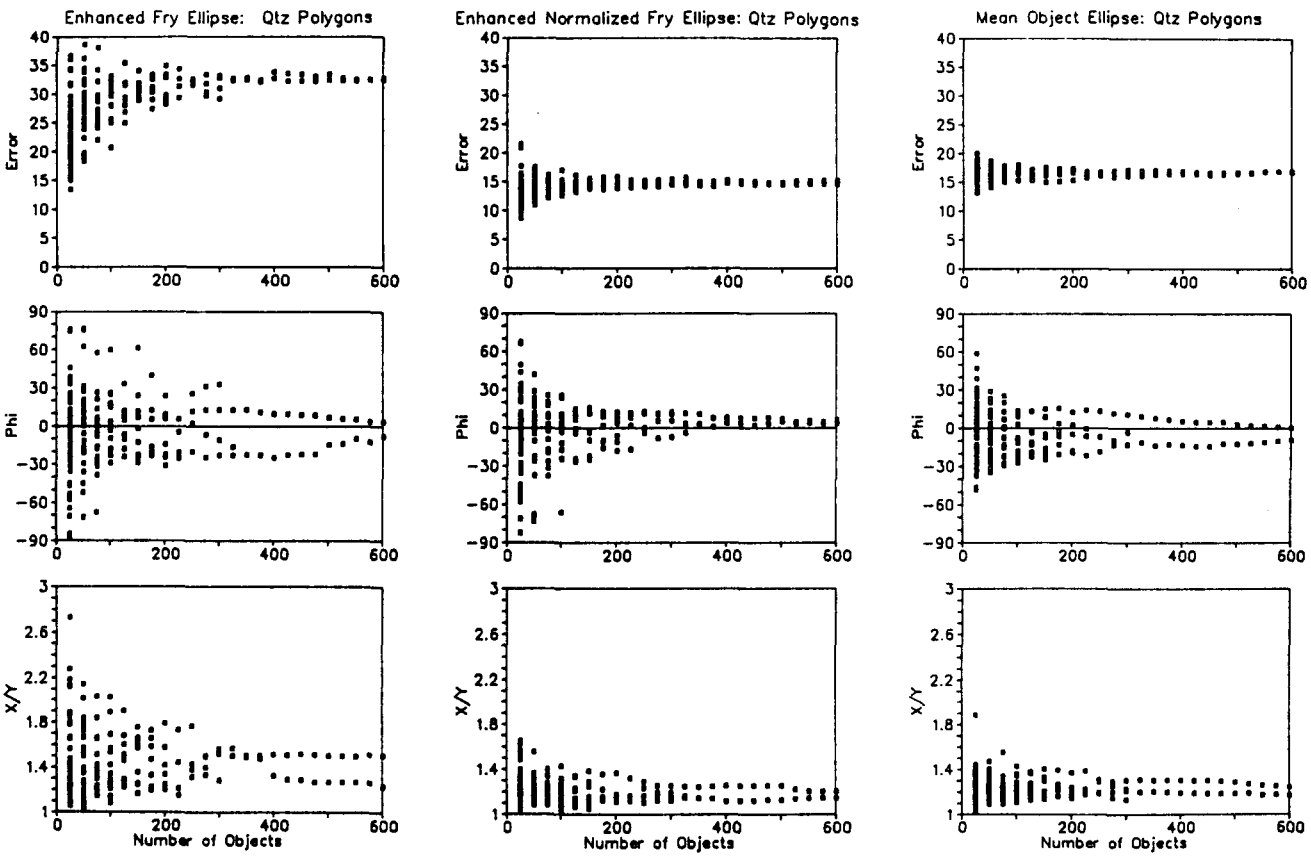

Fig. 9. Scatter plots of average radial error, long axis inclination and ellipticity for EFry, ENFry and MOE ellipse determinations using non-overlapping subsets of the polygonal quartz aggregate illustrated in Fig. 3(c).

sizes for an oolite and a quartz polygon subset. The other two subsets (another oolite and the quartz arenite in Fig. 3b) are analysed in Ge (1990) and summarized in Fig. 10. For all the methods, the range of values narrows considerably for subsets of 200 objects, giving a good estimate of the minimum number of objects needed for reasonable precision. The EFry method, which is dependent on the two-dimensional anticlustering of the aggregate, gives larger errors and results in more variable ellipticity and ϕ values. The MOE method is more precise than the ENFry method for smaller numbers of objects because each object contributes three points to the MOE least-squares algorithm whereas each object only contributes 0.6 points to the ENFry least-squares algorithm.

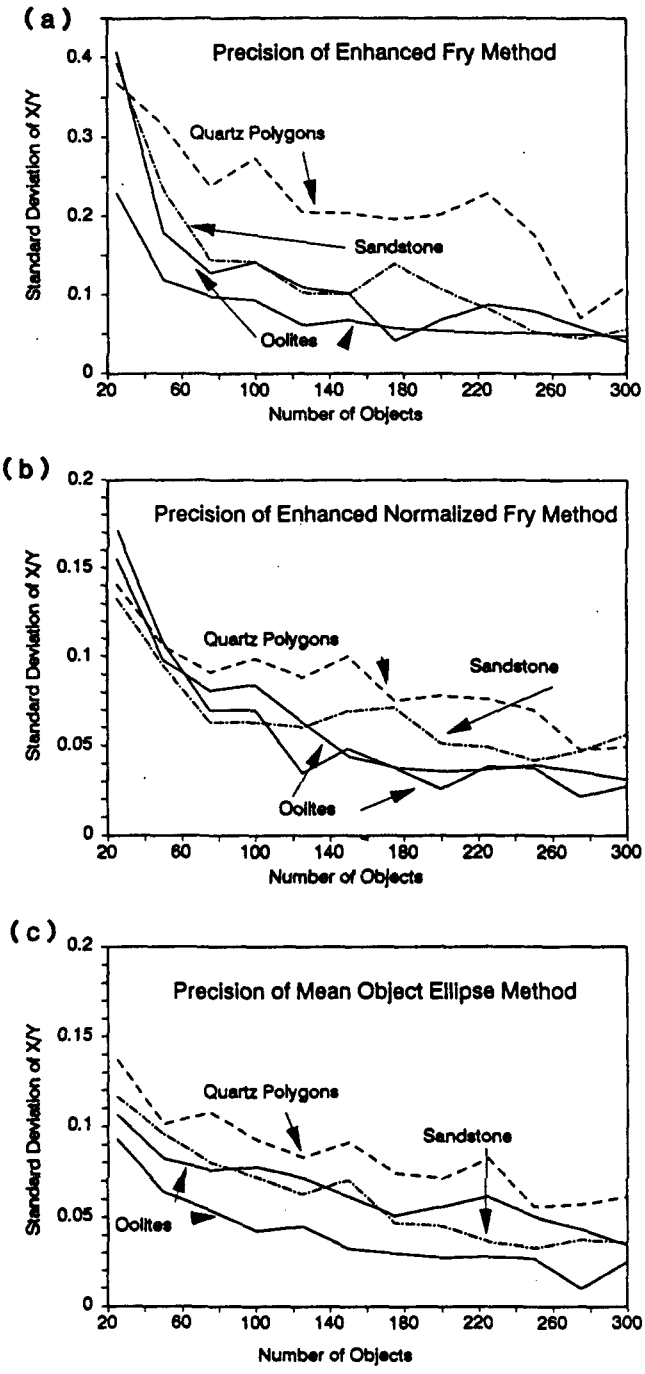

Fig. 10. Summary of the tests of precision (reproducibility) in Figs. 8 and 9, and Ge (1990). The standard deviation of each measure of ellipticity for subsets of 25–300 objects is plotted vs the number of objects in the data subset.

Figure 10 summarizes these precision measurements by plotting the standard deviation of the ellipticity vs the number of objects in the data set. MOE and ENFry methods are approximately twice as precise as the EFry method, which is clearly not the best choice for the analysis of packed aggregates. For large (>200 object) aggregates, MOE and ENFry give similar levels of precision, with all data sets giving standard deviations of ellipticity <0.1. For these methods, the oolitic limestones gave the lowest standard deviations of ellipticity, averaging <0.05 for aggregates with more than 200 objects.

The accuracy of fabric techniques is difficult to quantify from natural samples since we lack independent methods of determining the true fabric anisotropy. An alternate approach is to create an ideal, undeformed aggregate with a given range of initial ellipticity and then deform the aggregate by applying a stretching factor. Figure 11 shows two synthetic aggregates created using an ellipse template. These aggregates were copied by five rotations at 30° increments to increase the total number of objects and to assure random initial ellipse orientation. The samples were defined by five points on the margin of the ellipses, allowing incremental deformation of the objects by multiplying a stretch to the x coordinate of each point. Since the samples are not realistically anticlustered in two dimensions, the accuracy of the EFry method, which is dependent on the degree of anticlustering, cannot be evaluated.

The ratios of the strain values given by MOE, arithmetic mean ellipticity, harmonic mean ellipticity and ENFry methods to the synthetic deformation are plotted versus the synthetic deformation in Fig. 12 and summarized in Table 1. The harmonic and arithmetic mean ellipticities overestimate the strain, particularly at low synthetic strains where most of the object ellipticity is contributed by initial ellipticity. The MOE method correctly calculates the undeformed case yet overestimates the deformed case. This appears to be the result of the asymmetry of R_f values relative to the tectonic ellipticity. Since the tectonic ellipticity is closer to the minimum ellipticity than the maximum ellipticity, the strain is overestimated. The same effect causes some of the overestimation of strain by the arithmetic mean.

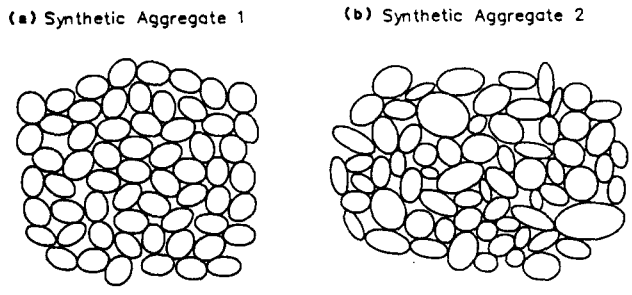

Fig. 11. Synthetic aggregates used to test the accuracy of the fabric methods.

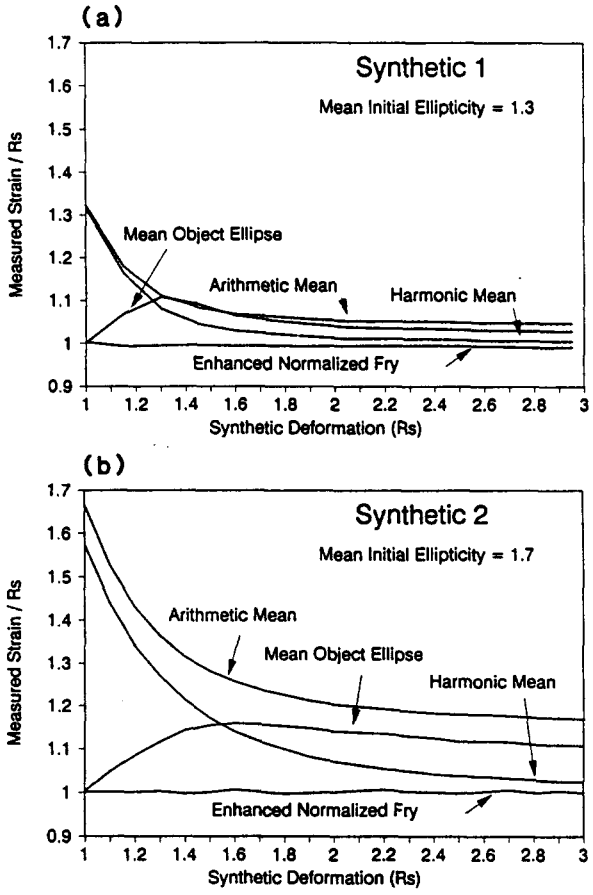

Fig. 12. The ratio of the measured ellipticity over the actual, synthetic deformation (R_s) plotted vs the synthetic deformation of the x dimensions. A perfect fabric method should always give a ratio of 1.0.

The ENFry method gives a close approximation of the actual strain in both cases. Of all the automated techniques, only the ENFry method gives errors which do not vary systematically with deformation. A simple manual implementation of the R_f/ϕ method gives accurate results for synthetic 1 but shows large errors for the more variable synthetic 2. This error (note the large standard deviations) reflects observer errors (E.A.E.) in the determination of $R_{f\,max}$ and $R_{f\,min}$.

This accuracy test assumes homogeneous deformation with identical object and matrix strain. Ideally, we would like to evaluate these strains separately. To test the effects of heterogeneous deformation, the program was modified so that the x-component of the center-to-center distance increased more than the actual deformation of initially circular objects. The resulting Fry and normalized Fry plots gave correct results for matrix deformation whereas MOE and mean ellipticities gave correct results for object deformation. However, the EFry and ENFry methods, implemented with automatic selection of touching pairs, gave least-squares ellipses intermediate between the object and matrix strains.

An analogous difference between matrix and object strains occurs in the ironstone oolites from fig. 7.7 of Ramsay & Huber (1983). Figure 13 shows two pairs of EFry and ENFry plots for this aggregate with different object-pair selection factors. The lower selection factor preferentially picks object pairs aligned parallel the the Y axis of the strain ellipse. Object pairs parallel to the X axis are not as readily selected since the larger matrix deformation has pulled them apart so they no longer 'touch' in the x direction. Thus, the EFry and ENFry least-squares ellipses calculated from object pairs selected by the computer do not give accurate estimations of the true matrix strain. If a sample population shows the radially biased selection of pairs seen in Fig. 13(a), a better estimate of matrix strain is given by manually fitting an ellipse to a normalized Fry plot.

The effect of spurious data on the strain methods is illustrated in Table 2 using a data set from fig. 5.7 of Ramsay & Huber (1983). It was acquired using an older version of the least-squares digitizing program which lacked comprehensive error checking. As a result, two spurious objects were defined with ellipticities of 38 and 11. Each spurious object contributed one additional center-to-center distance between 'touching' objects. MOE is particularly affected indicating that any spurious data will overwhelm the technique. The arithmetic mean ellipse is also strongly affected. The harmonic mean ellipticity and enhanced normalized Fry method show the least distortion. Since the harmonic mean sums the inverse ellipticities, the effect of large values is automatically minimized. The enhanced normalized Fry method requires two 'touching' objects with aligned spurious ellipticities to create an equally anomalous center-to-center distance. Thus, the effect of one spurious object is mitigated by the surrounding objects.

Table 1. Summary of accuracy tests

Method	Synthetic 1 (382 objects)* Average measured/strain (±1 SD)	Synthetic 1 (382 objects)* Total error‡ (%)	Synthetic 2 (408 objects)† Average measured/strain (±1 SD)	Synthetic 2 (408 objects)† Total error‡ (%)
Enhanced normalized Fry	0.9949 ± 0.0028	0.79	1.0015 ± 0.0025	0.40
Mean object ellipse	1.0475 ± 0.0269	7.44	1.1194 ± 0.0364	15.6
Harmonic mean	1.0525 ± 0.0840	13.6	1.1386 ± 0.1478	28.6
Arithmetic mean	1.0885 ± 0.0739	16.2	1.2636 ± 0.1293	39.3
R_f/ϕ§	1.0059 ± 0.0141	2.00	1.2018 ± 0.1380	34.0

*14 measurements at 0.15 R_s increments from 1.0 to 2.95 (Fig. 11a).
†21 measurements at 0.10 R_s increments from 1.0 to 3.0 (Fig. 11b).
‡Total error = 100 * (Absolute value (1 − average measured strain) + 1 SD).
§From manually measured $R_{f\,max}$ and $R_{f\,min}$ by E.A.E. on nine (synthetic 1) and seven (synthetic 2) R_f/ϕ plots.

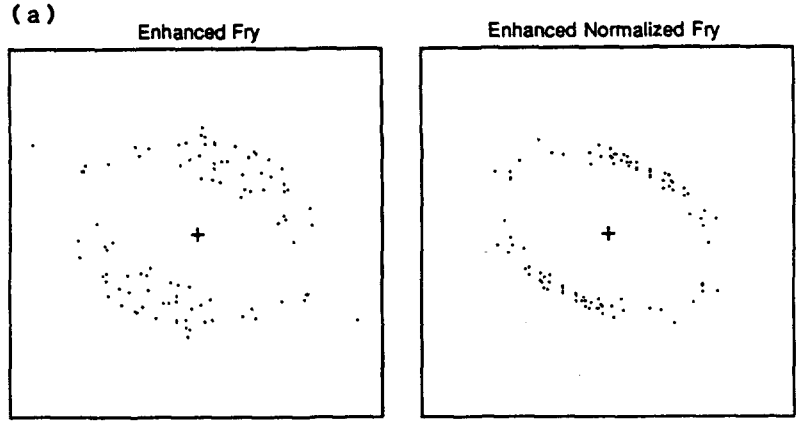

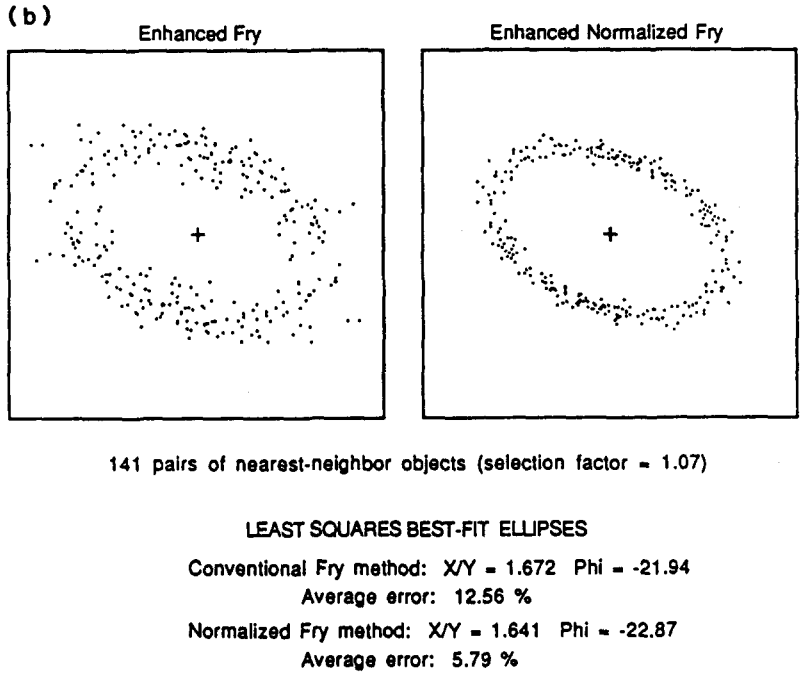

Fig. 13. Enhanced Fry (EFry) and enhanced normalized Fry (ENFry) plots of fig. 7.7 in Ramsay & Huber (1983) showing the effect of heterogeneous strain on the EFry and ENFry methods. Note the unequal radial distribution of points in ENFry plots, particularly at low selection factors.

Table 2. Effect of spurious data on quantitative fabric methods

		Files with spurious data	
Method	276 objects*	277 Objects*	278 Objects*
Maximum ellipticity	3.11	11.00	38.36
Rogue values	none	11.00	38.36, 11.00
Mean object ellipse	1.599	1.657	3.177
Arithmetic mean ellipticity	1.634	1.667	1.799
Harmonic mean ellipticity	1.568	1.573	1.578
Enhanced normalized Fry†	1.556	1.559	1.561

*Digitized ironstone ooids from fig. 5.7 of Ramsay & Huber (1983).
†Using an object-pair selection factor of 1.05.

CONCLUSIONS

Best-fit ellipse calculations can greatly increase the accuracy and precision of fabric analyses while reducing subjectivity. Accurate, unbiased approximation of an originally equant object outline as an ellipse is facilitated by least-squares ellipse fitting of digitized points on its margin. Angular grains require the input of more points than rounded grains for equivalent levels of precision.

The enhanced normalized Fry (ENFry) method calculates the best-fit ellipse through the rim of maximum point density of a normalized Fry diagram by only plotting distances between 'touching' pairs. The method is extremely accurate and precise for aggregates containing more than 200 objects. The ENFry method is also independent of variations in object size due to two-dimensional effects and sorting. The equivalent enhanced Fry (EFry) method gives at least twice the average radial error for packed aggregates and should only be used for populations with more highly developed two-dimensional anticlustering.

The mean object ellipse (MOE) method provides a high precision estimate of object shape. However, the use of a least-squares algorithm causes overestimation of object ellipticity due to the asymmetric distribution of object ellipses around the tectonic ellipticity. Ideally, a linear or least-square-root best-fit algorithm would lessen the influence of spurious and distal values of ellipticity. However, the least-squares MOE method does provide a good tool for fabric mapping because of its high precision in small data subsets.

The combination of automated, best-fit ellipse determination with quantitative methods of fabric analysis promises to provide new tools for a wide range of scientific investigations. The current concentration on strain analysis should be replaced with more generalized studies of fabric anisotropy.

Acknowledgements—We would like to thank William Dunne, Ana Vargo, Alfred Barnes, Roy Kligfield and Declan De Paor for their comments and insights. Reviews from David Sanderson, Bob Ratliff and an anonymous reviewer helped condense and clarify the manuscript. Acknowledgement is made to the Donors of the Petroleum Research Fund, administered by the American Chemical Society, for the support of this research.

REFERENCES

Bartlett, D. P. 1915. *General Principles of the Method of Least Squares With Applications*. Rumford Press, Concord, New Hampshire.

Bhattacharyya, T. & Longiaru, S. 1986. Ability of the Fry method to characterize pressure-solution deformation—Discussion. *Tectonophysics* **131**, 199–200.

Chilingarian, I. G. V. & Wolf, K. H. 1975. Diagenesis in sandstones and compaction. In: *Compaction of Coarse-grained Sediments* (edited by Chilingarian, I. G. V. & Wolf, K. H.). *Developments in Sedimentology*, **18B**. Elsevier, New York, 69–444.

Cloos, E. 1947. Oolite deformation in the South Mountain fold, Maryland. *Bull. geol. Soc. Am.* **58**, 843–918.

Crespi, J. M. 1986. Some guidelines for practical application of Fry's method of strain analysis. *J. Struct. Geol.* **8**, 799–808.

Dunnet, D. 1969. A technique of finite strain analysis using elliptical particles. *Tectonophysics* **7**, 117–136.

Erslev, E. A. 1988. Normalized center-to-center strain analysis of packed aggregates. *J. Struct. Geol.* **10**, 201–209.

Folk, R. L. 1974. *Petrology of Sedimentary Rocks*. Hemphill Publishing Co., Austin, Texas.

Fry, N. 1979. Random point distributions and strain measurement in rocks. *Tectonophysics* **60**, 806–807.

Ge, H. 1990. Quantitative center-to-center fabric analysis of homogeneous deformation. Unpublished M.S. thesis, Colorado State University.

Graton, L. C. & Fraser, H. J. 1935. Systematic packing of spheres—with particular reference to porosity and permeability. *J. Geol.* **43**, 785–909.

Lisle, R. J. 1977. Estimation of tectonic strain ratio from the mean shape of deformed elliptical markers. *Geol. Mijnb.* **56**, 140–144.

Lisle, R. J. 1985. *Geological Strain Analysis: A Manual for the R_f/ϕ Technique*. Pergamon Press, Oxford.

Panozzo, R. 1984. Two-dimensional strain from the orientation of lines in a plane. *J. Struct. Geol.* **6**, 215–221.

Powell, C. McA. 1982. Reduction of clastic grain size within cleavage zones. In: *Atlas of Deformational and Metamorphic Rock Fabrics* (edited by Borradaile, G. J., Bayly, M. B. & Powell, C. McA.). Springer-Verlag, Berlin, 302–303.

Ramsay, J. G. 1967. *Folding and Fracturing of Rocks*. McGraw-Hill, New York.

Ramsay, J. G. & Huber, M. I. 1983. *Techniques of Modern Structural Geology, Volume* 1: *Strain Analysis*. Academic Press, London.

Schmid, S. M., Panozzo, R. & Bauer, S. 1987. Simple shear experiments on calcite rocks: rheology and microfabric. *J. Struct. Geol.* **9**, 747–778.

Shimamoto, T. & Ikeda, Y. 1976. A simple algebraic method for strain estimation from deformed ellipsoidal objects. *Tectonophysics* **36**, 315–337.

Thomas, G. B. 1967. *Elements of Calculus and Analytical Geometry*. Addison-Wesley, Menlo Park, California.

APPENDIX

LEAST-SQUARES ALGORITHM FOR A CENTERED ELLIPSE

A general equation for conics, including ellipses, can be written as:

$$Ax^2 + Bxy + Cy^2 + Dx + Ey + F = 0. \quad \text{(A1)}$$

If $(B^2 - 4AC) \leq 0$, the equation (A1) describes an ellipse (Thomas 1967). If the elliptical pattern is centered on the origin, equation (A1) can be simplified to that of a centered conic:

$$Ax^2 + Bxy + Cy^2 - 1 = 0. \quad \text{(A2)}$$

For a given A, B and C, a point (x_a, y_a) will satisfy equation (A2) with the residual k_a defined by

$$k_a = Ax_a^2 + Bx_ay_a + Cy_a^2 - 1. \quad \text{(A3)}$$

If $k_a = 0$ and $(B^2 - 4AC) \leq 0$, the observed point (x_a, y_a) plots on the ellipse defined by constants A, B and C.

For an observed set of points (x_i, y_i), the sum of the squares of the deviations of the points from the best-fit ellipse can be minimized by minimizing the sum of the squares of the residual k_i (equation A4):

$$\text{Minimum} \sum (k_i^2) = \text{Minimum} \sum (Ax_i^2 + Bx_iy_i + Cy_i^2 - 1)^2. \quad \text{(A4)}$$

The conventional least-squares method (Bartlett 1915) can be applied to determine the coefficients A, B and C in the following way. First, equation (A4) is partially differentiated with respect to A, B and C and these equations are set to zero (equation A5):

$$\begin{aligned} d(\sum (k_i^2))/dA &= \sum (2 * (Ax_i^2 + Bx_iy_i + Cy_i^2 - 1) * x_i^2) = 0 \\ d(\sum (k_i^2))/dB &= \sum (2 * (Ax_i^2 + Bx_iy_i + Cy_i^2 - 1) * x_iy_i) = 0 \quad \text{(A5)} \\ d(\sum (k_i^2))/dC &= \sum (2 * (Ax_i^2 + Bx_iy_i + Cy_i^2 - 1) * y_i^2) = 0. \end{aligned}$$

These simplify to (A6):

$$A * \sum (x_i^4) + B * \sum (x_i^3 y_i) + C * \sum (x_i^2 y_i^2) = \sum (x_i^2)$$

$$A * \sum (x_i^3 y_i) + B * \sum (x_i^2 y_i^2) + C * \sum (x_i y_i^3) = \sum (x_i y_i) \quad \text{(A6)}$$

$$A * \sum (x_i^2 y_i^2) + B * \sum (x_i y_i^3) + C * \sum (y_i^4) = \sum (y_i^2).$$

Let

$$a = \sum (x_i^4), \quad b = \sum (x_i^3 y_i), \quad c = \sum (x_i^2 y_i^2),$$

$$d = \sum (x_i y_i^3), \quad e = \sum (y_i^4), \quad f = \sum (x_i^2), \quad \text{(A7)}$$

$$g = \sum (x_i y_i), \quad h = \sum (y_i^2)$$

and solve equations (A6)

$$A = \frac{(cef + cdg + bdh - c^2h - d^2f - beg)}{(ace + 2bcd - c^3 - ad^2 - b^2e)}$$

$$B = \frac{(aeg + bch + cdf - c^2g - adh - bef)}{(ace + 2bcd - c^3 - ad^2 - b^2e)} \quad \text{(A8)}$$

$$C = \frac{(ach + bdf + cbg - c^2f - b^2h - adg)}{(ace + 2bcd - c^3 - ad^2 - b^2e)}.$$

The resulting A, B and C are the coefficients of the least-squares best-fit ellipse. The ellipticity and inclination of the long axis can be solved using analytical geometry (Thomas 1967).